45° sign switching of effective exchange bias due to competing anisotropies in fully epitaxial Co_3FeN/MnN bilayers

T Hajiri[1], T Yoshida[1], M Filianina[2], S Jaiswal[2,3], B Borie[2,4], H Asano[1], H Zabel[2], M. Kläui[2]

[1] Department of Materials Physics, Nagoya University, Nagoya 464-8603, Japan
[2] Institut für Physik, Johannes Gutenberg-Universität Mainz, Staudingerweg 7, Mainz, D-55128, Germany
[3] Singulus Technologies AG, Kahl am Main, D-63796, Germany
[4] Sensitec GmbH, Hechtsheimer Str. 2, Mainz, D-55131, Germany

E-mail: t.hajiri@numse.nagoya-u.ac.jp

October 2017

Abstract. We report an unusual angular-dependent exchange bias effect in ferromagnet/antiferromagnet bilayers, where both ferromagnet and antiferromagnet are epitaxially grown. Numerical model calculations predict an approximately 45° period for the sign switching of the exchange-bias field, depending on the ratio between magnetocrystalline anisotropy and exchange-coupling constant. The switching of the sign is indicative of a competition between a fourfold magnetocrystalline anisotropy of the ferromagnet and a unidirectional anisotropy field of the exchange coupling. This predicted unusual angular-dependent exchange bias and its magnetization switching process are confirmed by measurements on fully epitaxial Co_3FeN/MnN bilayers by longitudinal and transverse magneto-optic Kerr effect magnetometry. These results provide a deeper understanding of the exchange coupling phenomena in fully epitaxial bilayers with tailored materials and open up a complex switching energy landscape engineering by anisotropies.

Keywords: exchange coupling, magnetization switching process, magnetic anisotropy
Submitted to: *J. Phys.: Condens. Matter*

1. Introduction

Exchange coupling between ferromagnets (FMs) and antiferromagnets (AFMs) is one of the important phenomena in spintronic devices [1, 2]. In addition, FM/AFM bilayers have recently attracted much attention in AFM spintronics where AFM layers play a leading role similar to FM layers in FM spintronics [3, 4, 5], because AFM

moments can be controlled via exchange-coupled FMs [6, 7, 8, 9]. Since AFM materials have the advantage of much faster spin dynamics [10, 11], better stability against external field perturbations [12], and no stray field [13, 14] compared with FM, FM/AFM bilayers are preferred in spintronic device applications. On the other hand, the FM magnetocrystalline anisotropy affects rotating AFM moments via exchange-spring effect [6] in FM/AFM, suggesting that AFM moments can be controlled by anisotropies [9].

The main properties of exchange coupling are well understood such as the shift of hysteresis loops and the broadening of coercive fields [15, 16, 17] for, in particular, polycrystalline bilayers [16, 18, 19]. In the case of full epitaxial FM/AFM bilayers, the situation is more complex because of unusual magnetization switching processes resulting from competing anisotropies between a fourfold magnetocrystalline anisotropy and a unidirectional exchange coupling [17, 20, 21, 22, 23, 24, 25]. Although the unusual magnetization switching model has been well defined as 90° domain wall nucleation and propagation [20, 26], so far there have been no studies discussing the effect of unusual magnetization processes due to competing anisotropies on the exchange coupling. However, only epitaxial growth allows us to explore more exciting magnetic properties [17], such as high spin polarization [27] and Néel order spin orbit torque [28, 29, 30]. Thus, there is a clear need to study high-quality heteroepitaxial structures. Besides, the magnitude of an uniaxial or a biaxial magnetic anisotropy can be tuned by using the magnetoelectric effect [31, 32, 33], which allows for flexible manipulation of the magnetization switching energy. Therefore, the deep understanding of the magnetization switching energy landscape induced by competing anisotropies is necessary in order to harness this flexibility for novel spintronics devices.

Our previous study clarified the unusual magnetization switching process and its angular-dependent exchange bias in fully epitaxial bilayers using Co_3FeN (CFN) for FM and MnN for AFM. CFN is theoretically expected to be a half-metallic ferromagnet (FM) with a negative spin polarization [34, 35]. MnN exhibits a high Néel temperature of 640 K in spite of without rare metals [36, 37]. Field cooling (FC) was carried out along the easy axis of the fourfold magnetocrystalline anisotropy of CFN [38]. In this situation, the magnetization switching process and angular-dependent exchange bias of those bilayers can be reproduced by combining a Stoner-Wohlfarth model and a 90° domain wall nucleation and propagation model [38]. However, our previous study only dealt with FC along the easy axis of CFN. Moreover, although there are several studies which reveal unusual magnetization switching process in fully epitaxial stacks [20, 21, 22, 23, 24, 25, 26], there are no studies where FC is applied parallel to the hard axis. However it is exactly the hard-axis direction, which can lead to the most complex switching behaviors. In fact, small bifurcations from the hard-axis direction can lead to large changes in the resulting switching. Therefore, not only angular-dependent exchange bias but also magnetization switching behavior in more complex cases where FC is applied along a direction parallel to the hard axis still remains unexplored.

In this work, we predict a new unusual angular-dependent exchange-bias resulting

from the special magnetization switching behavior due to the competition between fourfold magnetocrystalline anisotropy and unidirectional anisotropy field of the exchange coupling. In contrast to our previous study where FC was carried out along the easy axis of fourfold magnetocrystalline anisotropy, the angular-dependent exchange bias exhibits an approximately 45° period for the sign switching of the exchange bias field as predicted in numerical calculations, where FC is applied along the hard axis. Experimentally determined magnetization switching process by magneto-optic Kerr effect (MOKE) magnetometry is consistent with our predictions, highlighting the essential role of the competition between magnetocrystalline anisotropy and exchange coupling. These results could provide a deeper understanding of exchange-coupling phenomena of fully epitaxial bilayers with competing anisotropies.

2. Experimental details

High-quality epitaxial CFN (5 nm)/MnN (30 nm) bilayers were prepared by reactive magnetron sputtering on $MgAl_2O_4$ substrates, as described elsewhere [38]. The bilayers were capped with 3 nm Hf layer to prevent oxidation. Each film thickness is evaluated from the growth rate, which is calibrated by a Dektak profiler prior to bilayer growth. After bilayer growth, we obtained the exchange bias by annealing at 400 °C for 30 minutes in a field of 150 mT along CFN/MnN [100], subsequentially cooling to room temperature in the same field and pointing in the same direction. We have characterized the magnetic properties via the magneto-optic Kerr effect using longitudinal (L-MOKE) and transverse geometries (T-MOKE), respectively. L-MOKE measurements were carried out using a red (635 nm) low noise laser diode to determine the angular-dependent H_{ex}. On the other hand, T-MOKE magnetometry was performed by using a Kerr microscope to evaluate the magnetization switching process. The schematics of both MOKE setups are shown in Fig. 1. All MOKE magnetometry measurements were recorded at room temperature. The model and experimental configuration is shown in Fig. 3(a).

3. Stonar-Wolfarth model calculation

Figures 2(a)-2(d) show the schematic magnetization switching processes of as grown CFN/MnN case [38]. The magnetization switching process shows 5 steps from the positive (negative) to negative (positive) field sweep. In all cases, the magnetization switches by passing through the easy axes E2 or E4. In this situation, a Stoner-Wolfarth model can be adapted [38] and expressed as

$$\begin{aligned} E = &-\mu_0 M_s H t_F \cos\theta + t_F K_{u,ex} \sin^2(\theta - \theta_{u,ex}) \\ &+ t_F K_1 \sin^2(\theta - \theta_c)\cos^2(\theta - \theta_c) - J_{ex}\sin\theta. \end{aligned} \tag{1}$$

Here $K_{u,ex}$ and K_1 are the uniaxial anisotropy and the fourfold magnetocrystalline anisotropy, respectively, θ is the angle between the magnetization and the applied

field direction, $\theta_{u,ex}$, θ_c and θ_{FC} are the angles between the uniaxial anisotropy and applied field direction, between the fourfold magnetocrystalline anisotropy and applied field direction, and between the FC and applied field direction, respectively, J_{ex} is the exchange coupling constant [39, 38].

When FC is carried out along E1, the sign of exchange-coupling term [$J_{ex}\sin(\theta)$] of Eq. 1 is reversed along the E2–E4 line as shown in Fig. 2(e), indicating that the exchange-coupling term becomes 0 before its sign is reversed. On the other hand, when FC is applied along any of the hard axes $\langle 100\rangle$, the sign of the exchange-coupling term is reversed along the $\langle 010\rangle$–$\langle$0-10$\rangle$ line as shown in Fig. 2(f), indicating that the exchange-coupling term does not become 0 before its sign reversed. Since the change of exchange-coupling term for FC parallel to the hard axis case is larger than that of FC parallel to the easy axis case, this might lead to more complex angular dependencies. Thus, we focus on the case of the FC along the hard axis configuration as shown in Fig. 3(a). We note that the direction $K_{u,ex}$ is perpendicular to FC due to noncollinear FC or interfacial frustration [40, 41] as clarified in our previous paper [38].

Figure 3(b) shows the series of calculated angular-dependent H_{ex} using a constant $K_1 = 20000$ J/m^3 and $K_u = 0$ J/m^3. For $J_{ex}/t_F = 5000$ J/m^3, the maximum H_{ex} appears around $\theta = 40°$. At $\theta = 45°$, the exchange bias shows an abrupt sign change and a negative H_{ex} appears between $\theta = 45°$ and 90°. A positive H_{ex} occurs between $\theta = 90°$ and 135°, and a negative H_{ex} appears again between $\theta = 135°$ and 180°. Therefore, the angular dependence shows a sign switching with a 45° periodicity (State 1). This feature is clearly distinct from the angular dependence of polycrystalline bilayers and from full epitaxial bilayer with FC along the easy axis. The origin of an abrupt sign change and a 45° periodicity of H_{ex} will be discussed later. In the latter case, a 180° period sign switching is observed. At $J_{ex}/t_F = 10000$ J/m^3, the maximum exchange bias increases and the anomalous H_{ex} area around $\theta = 40, 120°$, becomes narrower. For further increasing J_{ex}/t_F, the maximum exchange bias increases as well and the anomalous H_{ex} area disappears (State 2). The angular-dependent H_{ex} feature is summarized in Fig. 3(c) as a function of J_{ex}/t_F, K_1 and K_u. As clearly seen, there is a proportional relation between J_{ex}/t_F and K_1. Then, the border between State 1 (red circles) and State 2 (blue crosses) due to $(J_{ex}/t_F)/K_1$ ratio is changed by K_u, indicating that the anomalous exchange bias originates from the competition of these anisotropies according to our model calculations.

4. MOKE results and discussion

Figure 4(a) shows the series of angular-dependent L-MOKE loops after FC along CFN [100], which is a hard axis direction. Fourfold easy and hard axes MOKE loops are found along $\theta = 45, 135°$ (easy axes) and 90° (hard axis), respectively. Most loops exhibit a multistep feature. The step positions H_{step} as indicated by arrows in Fig. 4(a) are plotted (open circle) in Fig. 4(b). The multistep position shows approximately a fourfold symmetry, which is a similar feature as for the as-grown case, suggesting that multistep

reversal can be related to the fourfold magnetocrystalline anisotropy [26, 38]. To acquire the exchange-coupling constant and uniaxial anisotropy due to FC [40, 41], we modified the 90° domain wall nucleation and propagation model [26, 38]. The 90° domain wall nucleation and propagation model is based on total energy minimization [26, 20]. When the unidirectional anisotropy E_{ex} due to exchange coupling and the uniaxial anisotropy $K_{u,ex}$ are non-collinear with fourfold magnetocrystalline anisotropy as shown in Fig. 5, the energies of single domain states which are directed to each fourfold easy axis can be expressed as

$$\begin{aligned}
E_{E1} &= -\mu_0 M_s H\cos\phi - E_{ex}\cos\alpha + K_{u,ex}\sin\beta, \\
E_{E2} &= -\mu_0 M_s H\sin\phi - E_{ex}\sin\alpha + K_{u,ex}\cos\beta, \\
E_{E3} &= \mu_0 M_s H\cos\phi + E_{ex}\cos\alpha + K_{u,ex}\sin\beta, \\
E_{E4} &= \mu_0 M_s H\sin\phi + E_{ex}\sin\alpha + K_{u,ex}\cos\beta,
\end{aligned} \tag{2}$$

Here, M_s is the saturation magnetization and ϕ, α, β are the angles between applied field and the easy axis E1, between the unidirectional anisotropy E_{ex} and E1, and between the uniaxial anisotropy $K_{u,ex}$ and E1, respectively, as defined in Fig. 5. The switching fields between two easy axis directions of the fourfold anisotropy can be obtained from the total energy minima and expressed by following equations;

$$\begin{aligned}
\mu_0 H_{E1\to E2} &= \frac{E_{1\to 2} - E_{ex}(\sin\alpha - \cos\alpha) - K_{u,ex}(\sin\beta - \cos\beta)}{M_s(\sin\theta - \cos\theta)}, \\
\mu_0 H_{E2\to E3} &= \frac{E_{2\to 3} + E_{ex}(\sin\alpha + \cos\alpha) + K_{u,ex}(\sin\beta - \cos\beta)}{M_s(-\sin\theta - \cos\theta)}, \\
\mu_0 H_{E3\to E4} &= \frac{E_{3\to 4} + E_{ex}(\sin\alpha - \cos\alpha) - K_{u,ex}(\sin\beta - \cos\beta)}{M_s(-\sin\theta + \cos\theta)}, \\
\mu_0 H_{E4\to E1} &= \frac{E_{4\to 1} - E_{ex}(\sin\alpha + \cos\alpha) + K_{u,ex}(\sin\beta - \cos\beta)}{M_s(\sin\theta + \cos\theta)}, \\
\mu_0 H_{E1\to E4} &= \frac{E_{1\to 4} + E_{ex}(\sin\alpha + \cos\alpha) - K_{u,ex}(\sin\beta - \cos\beta)}{M_s(-\sin\theta - \cos\theta)}, \\
\mu_0 H_{E4\to E3} &= \frac{E_{4\to 3} - E_{ex}(\sin\alpha - \cos\alpha) - K_{u,ex}(\sin\beta - \cos\beta)}{M_s(\sin\theta - \cos\theta)}, \\
\mu_0 H_{E3\to E2} &= \frac{E_{3\to 2} - E_{ex}(\sin\alpha + \cos\alpha) + K_{u,ex}(\sin\beta - \cos\beta)}{M_s(\sin\theta + \cos\theta)}, \\
\mu_0 H_{E2\to E1} &= \frac{E_{2\to 1} + E_{ex}(\sin\alpha - \cos\alpha) - K_{u,ex}(\sin\beta - \cos\beta)}{M_s(-\sin\theta + \cos\theta)}
\end{aligned} \tag{3}$$

Here $H_{E1\to E2}$ and $E_{1\to 2}$ are the switching field and the domain wall nucleation energy from easy axis E1 to easy axis E2, respectively. Since ϕ, α and β are $\theta + 45°, -45°$ and 45°, respectively, in this study, all $K_{u,ex}$ terms become 0 in the 90° domain wall nucleation and propagation model.

As shown by the solid line in Fig. 4(b), the step positions can be reproduced well by the 90° domain wall nucleation and propagation model. In the same manner with FC along the easy axis, J_{ex}/t_F is evaluated for 8000 J/m^3, using the fourfold magnetocrystalline anisotropy 33700 J/m^3 of CFN [38]. On the other hand, as shown in Fig. 3(c), $K_{u,ex}$ affects the magnetization switching process and H_{ex} because the magnetization does not perfectly rotate towards the easy axes, as shown in Fig. 2(a)–2(d). Thus, $K_{u,ex}$ is estimated for 2450 J/m^3 from the ratio between J_{ex}/t_F and $K_{u,ex}$ of FC along the easy axis case [38]. We should note that when the anisotropies compete, also 180° domain wall processes may appear [26, 21]. However, since there is no clear 180° domain wall process behavior in our work in contrast to the one reported in Ref. [21] in Fig. 4(b), we only consider the 90° domain wall process.

Finally, we turn our attention to the angular-dependent exchange bias field H_{ex}. Figure 6(a) shows the angular-dependent H_{ex} of CFN/MnN bilayers obtained from L-MOKE loops. The sign of H_{ex} changes in 45° periods, which is expected in our model calculation as shown in Fig. 3(a). The calculated angular-dependent H_{ex} is shown in Fig. 6(a) using $K_1 = 33700$ J/m^3, $K_{u,ex} = 2450$ J/m^3 and $J_{ex}/t_F = 8000$ J/m^3 determined by the 90° domain wall nucleation and propagation model along with the experimental result. The calculations reproduce the experimental angular dependence reasonably well, while the calculated H_{ex} is found to be an order of magnitude larger than experimental one. Although our model calculation treats only the competing anisotropies, other factors such as interface frustration and roughness are known to affect the exchange coupling [40, 42]. Therefore, the discrepancy of an order of magnitude of H_{ex} between calculation and experiment might originate from these factors.

The comparison between experimental and calculated angular-dependent T-MOKE loops is shown in Fig. 6(b). The calculated T-MOKE loops agree fairly well with experimental T-MOKE loops. These angular-dependent T-MOKE loops indicate that the magnetization switching processes of Fig. 2(a) for $\theta = 0 \sim 45°$ and Fig. 2(b) for $\theta = 45 \sim 90°$ are realized in this system. This different magnetization switching affects when the sign of the exchange-coupling term $[J_{ex}\sin(\theta)]$ of Eq. 1 changes during the magnetization switching; for $\theta = 0 \sim 45°$, the sign of $J_{ex}\sin(\theta)$ changes at second magnetization jump [from E1 to E2, see Fig. 2(a)], while the sign of $J_{ex}\sin(\theta)$ changes at third magnetization jump for $\theta = 0 \sim 45°$ [from E4 to E3, see Fig. 2(b)]. Besides, as discussed in Fig. 2(f), the change of $J_{ex}\sin(\theta)$ is large when its sign changes. These facts demonstrate that the large and different sign change of $J_{ex}\sin(\theta)$ during the magnetization switching process between $\theta = 0 \sim 45°$ and $\theta = 45 \sim 90°$ is the origin of an abrupt sign change around $\theta = 45°$ and a 45° periodicity of H_{ex}. Furthermore, the magnetization switching process is consistent with those expected by the 90° domain wall nucleation and propagation model as shown in Fig. 4(b). Thus, estimated anisotropies K_1, $K_{u,ex}$ and J_{ex}/t_F by the 90° domain wall nucleation and propagation model are reasonable values and the predicted 45° sign switching of H_{ex} is experimentally clarified.

5. Conclusion

We predict a 45° period for the sign switching of the angular-dependent exchange-bias field H_{ex} for FC along the hard axis of an epitaxial FM/AFM bilayer system. Experimentally we have confirmed this periodicity in fully epitaxial CFN/MnN bilayers using MOKE magnetometry measurements. The numerical model calculation based on a Stoner-Wohlfarth model indicates the effect of competing anisotropies leading to complex switching behavior. Taking into account the experimentally determined anisotropy constants by the modified 90° domain wall nucleation and propagation model, the predicted and experimentally obtained 45° period for the sign switching of angular-dependent H_{ex} is reproduced well. Moreover, the magnetization switching process is reproduced as well, demonstrating that unusual 45° period sign switching of angular-dependent H_{ex} is attributable to unusual magnetization switching due to competing anisotropies. These results highlight the intricate interplay of the exchange-coupling phenomena leading to a complex angular dependence of the switching behavior in fully epitaxial bilayers. Furthermore, these results open up possibilities for artificially tuning of the exchange-coupling phenomena by competing anisotropies, providing a guide to applications by using fully epitaxial stacks with tailored materials.

6. Acknowledgments

This work was supported by Japan Society for the Promotion of Science (JSPS) Program for Advancing Strategic International Networks to Accelerate the Circulation of Talented Researchers, JSPS KAKENHI Grant Number 17K17801 and 17K19054, the Center for Spintronics Research Network (CSRN) of Tohoku University, The Murata Science Foundation, the Deutsche Forschungsgemeinschaft (DFG, SFB TRR 173 Spin+X in particular the visiting guest researcher program), and the Graduate School of Excellence Materials Science in Mainz (GSC 266). S.J., B.B., and M.K. gratefully acknowledge the European Union for funding under the FP7 Marie Curie ITN WALL project/Grant No. FP7-PEOPLE-2013-ITN 608031.

7. References

[1] Wolf S A, Awschalom D D, Buhrman R A, Daughton J M, Molnár S, Roukes M L, Chtchelkanova A Y, and Treger D M 2001 Spintronics: A Spin-Based Electronics Vision for the Future *Science* **294** 1488

[2] Åkerman J 2005 Toward a Universal Memory *Science* **308** 508

[3] Gomonay E V and Loktev V M 2014 Spintronics of antiferromagnetic systems *LowTemp.Phys.* **40** 17

[4] Jungwirth T, Martí X, Wadley P and Wunderlich J 2016 Antiferromagnetic spintronics *Nat.Nanotech.* **11** 231

[5] Baltz V, Manchon A, Tsoi M, Moriyama T, Ono T, and Tserkovnyak Y 2016 Antiferromagnetic spintronics *arXiv*:1606.04284

[6] Scholl A, Liberati M, Arenholz E, Ohldag H, and Stöhr J 2004 Creation of an Antiferromagnetic Exchange Spring *Phys.Rev.Lett.* **92** 247201

[7] Park B G, Wunderlich J, Martí X, Holý V, Kurosaki Y, Yamada M, Yamamoto H, Nishide A, Hayakawa J, Takahashi H, Shick A B, and Jungwirth T 2011 A spin-valve-like magnetoresistance of an antiferromagnet-based tunnel junction *Nat.Mater.* **10** 347

[8] Sakakibara H, Ando H, Kuroki Y, Kawai S, Ueda K, and Asano H 2015 Magnetic properties and anisotropic magnetoresistance of antiperovskite nitride Mn_3GaN/Co_3FeN exchange-coupled bilayers *J.Appl.Phys.* **117** 17D725

[9] Hajiri T, Matsushita M, Ni Y Z, and Asano H, 2017 Impact of anisotropy on antiferromagnet rotation in Heusler-type ferromagnet/antiferromagnet epitaxial bilayers *Phys.Rev.B* **95** 134413

[10] Kimel A V, Kirilyuk A, Tsvetkov A, Pisarev R V, and Rasing T 2004 Laser-induced ultrafast spin reorientation in the antiferromagnet $TmFeO_3$ *Nature* **429** 850

[11] Železný J, Gao H, Výborný K, Zemen J, Mašek J, Manchon A, Wunderlich J, Sinova J, and Jungwirth T 2014 Relativistic Néel-Order Fields Induced by Electrical Current in Antiferromagnets *Phys.Rev.Lett.* **113** 157201

[12] Kriegner D, Výborný K, Olejník K, Reichlová H, Novák V, Martí X, Gazquez J, Saidl V, Němec P, Volobuev V V, Springholz G, Holý V, and Jungwirth T 2016 Multiple-stable anisotropic magnetoresistance memory in antiferromagnetic MnTe *Nat.Commun.* **7** 11623

[13] Loth S, Baumann S, Lutz C P, Eigler D M, and Heinrich A J 2012 Bistability in Atomic-Scale Antiferromagnets *Science* **335** 196

[14] Petti D, Albisetti E, Reichlová H, Gazquez J, Varela M, Molina-Ruiz M, Lopeandía A F, Olejník K, Novák V, Fina I, Dkhil B, Hayakawa J, Martí X, Wunderlich J, Jungwirth T, and Bertacco R 2013 Storing magnetic information in IrMn/MgO/Ta tunnel junctions via field-cooling *Appl.Phys.Lett.* **102** 192404

[15] Nogués J and Schuller I K 1999 Exchange bias *J.Magn.Magn.Mater.* **192** 203–232

[16] Radu F and Zabel H, 2008 Exchange Bias Effect of Ferro-/Antiferromagnetic Heterostructures *Magnetic Heterostructures*, *SpringerTractsinModernPhysics* (Springer, Berlin) **227** 97-184.

[17] Zhanga W and Krishnan K M 2016 Epitaxial exchange-bias systems: From fundamentals to future spin-orbitronics *Mater.Sci.Eng.R* **105** 1–20

[18] Camarero J, Sort J, Hoffmann A, García-Martín J M, Dieny B, Miranda R, and Nogués J 2005 Origin of the Asymmetric Magnetization Reversal Behavior in Exchange-Biased Systems: Competing Anisotropies *Phys.Rev.Lett.* **95** 057204

[19] Radu F, Westphalen A, Theis-Bröhl K, and Zabel H 2006 Quantitative description of the azimuthal dependence of the exchange bias effect *J.Phys.Condens.Matter* **18** L29–L36

[20] Arenholz E and Liu K 2005 Angular dependence of the magnetization reversal in exchange-biased Fe/MnF_2 *Appl.Phys.Lett.* **87** 132501

[21] Zhang W, Bowden M E, and Krishnan K M 2011 Competing effects of magnetocrystalline anisotropy and exchange bias in epitaxial Fe/IrMn bilayers *Appl.Phys.Lett.* **98** 092503

[22] Zhang W and Krishnan K M 2012 Domain wall nucleation in epitaxial exchange-biased Fe/IrMn bilayers with highly misaligned anisotropies *J.Magn.Magn.Mater.* **324** 3129–3132

[23] Zhan Q F and Krishnan K M 2010 Angular dependence of magnetization reversal process in exchange biased epitaxial MnPd/Fe bilayers *J.Appl.Phys.* **107** 09D703

[24] Zhan Q F, Zhang W, and Krishnan K M 2011 Antiferromagnetic layer thickness dependence of the magnetization reversal in the epitaxial MnPd/Fe exchange bias system *Phys.Rev.B* **83** 094404

[25] Zhang Y, Zhan Q, Zuo Z, Yang H, Zhang X, Dai G, Liu Y, Yu Y, Wang J, Wang B, and Li R W 2015 Magnetization reversal in epitaxial exchange-biased IrMn/FeGa bilayers with anisotropy geometries controlled by oblique deposition *Phys.Rev.B* **91** 174411

[26] Cowburn R P, Gray S J, and Bland J A C 1997 Multijump Magnetic Switching in In-Plane Magnetized Ultrathin Epitaxial Ag/Fe/Ag(001) Films *Phys.Rev.Lett.* **79** 4018

[27] Jourdan M, Minár J, Braun J, Kronenberg A, Chadov S, Balke B, Gloskovskii A, Kolbe M, Elmers H J, Schönhense G, Ebert H, Felser C, and Kläui M 2014 Direct observation of half-metallicity in the Heusler compound Co_2MnSi *Nat.Commun.* **5** 3974

[28] Wadley P, Howells B, Železný J, Andrews C, Hills V, Campion R P, Novák V, Olejnik K,

Maccherozzi F, Dhesi S S, Martin S Y, Wagner T, Wunderlich J, Freimuth F, Mokrousov Y, Kuneš J, Chauhan J S, Grzybowski M J, Rushforth A W, Edmonds K W, Gallagher B L, and Jungwirth T 2015 Electrical switching of an antiferromagnet *Science* **351** 587

[29] Gomonay O, Jungwirth T, and Sinova J 2016 High Antiferromagnetic Domain Wall Velocity Induced by Néel Spin-Orbit Torques O. *Phys.Rev.Lett.* **117** 017202

[30] Bodnar S Y, Šmejkal L, Turek I, Jungwirth T, Gomonay O, Sinova J, Sapozhnik A A, Elmers H J, Kläui M, and Jourdan M 2017 Writing and Reading antiferromagnetic Mn_2Au: Néel spin-orbit torques and large anisotropic magnetoresistance. *arXiv*:1706.02482

[31] Parkes D E, Cavill S A, Hindmarch A T, Wadley P, McGee F, Staddon C R, Edmonds K W, Campion R P, Gallagher B L, and Rushforth A W 2012 Non-volatile voltage control of magnetization and magnetic domain walls in magnetostrictive epitaxial thin films *Appl.Phys.Lett.* **101** 072402

[32] Wu T, Bur A, Wong K, Hockel J L, Hsu C J, Kim H K D, Wang K L, and Carman G P 2011 Electric-poling-induced magnetic anisotropy and electric-field-induced magnetization reorientation in magnetoelectric Ni/(011) $[Pb(Mg_{1/3}Nb_{2/3})O_3]_{(1-x)}$-$[PbTiO_3]_x$ heterostructure *J.Appl.Phys.* **109** 07D732

[33] Finizio S, Foerster M, Buzzi M, Krüger B, Jourdan M, Vaz C A F, Hockel J, Miyawaki T, Tkach A, Valencia S, Kronast F, Carman G P, Nolting F, and Kläui M 2014 Magnetic Anisotropy Engineering in Thin Film Ni Nanostructures by Magnetoelastic Coupling *Phys.Rev.Appl.* **1** 021001

[34] Takahashi Y, Imai Y, and Kumagai T 2011 Spin-polarized electronic band structures of the Fe_4N-Co_4N system Yasuhiko *J.Magn.Magn.Mater.* **323** 2941

[35] Gushi T, Ito K, Honda S, Yasutomi Y, Toko K, Oosato H, Sugimoto Y, Asakawa K, Ota N, and Suemasu T 2015 Fabrication of L-shaped Fe_4N ferromagnetic narrow wires and position control of magnetic domain wall with magnetic field *Jpn.J.Appl.Phys.* **54** 028003

[36] Suzuki K, Kaneko T, Yoshida H, Obi Y, Fujimori H, and Morita H 2000 Crystal structure and magnetic properties of the compound MnN *J.AlloysCompd.* **306** 66–71

[37] Meinert M, Büker B, Graulich D, and Dunz M 2015 Large exchange bias in polycrystallineMnN/CoFe bilayers at room temperature *Phys.Rev.B* **92** 144408

[38] Hajiri T, Yoshida T, Jaiswal S, Filianina M, Borie B, Ando H, Asano H, Zabel H, and Kläui M 2016 Magnetization switching behavior with competing anisotropies in epitaxial Co_3FeN/MnN exchange-coupled bilayers *Phys.Rev.B* **94** 184412

[39] Bai Y and Xu X 2015 The Effect of Fourfold Anisotropy on the Angular Dependence of the Exchange Bias *IEEETrans.Magn.* **11** 4800404

[40] Jiménez E, Camarero J, Sort J, Nogués J, Mikuszeit N, García-Martín J M, Hoffmann A, Dieny B, and Miranda R 2009 Emergence of noncollinear anisotropies from interfacial magnetic frustration in exchange-bias systems *Phys.Rev.B* **80** 014415

[41] Jiménez E, Camarero J, Sort J, Nogués J, Hoffmann A, Teran F J, Perna P, García-Martín J M, Dieny B, and Miranda R 2009 Highly asymmetric magnetic behavior in exchange biased systems induced by noncollinear field cooling *Appl.Phys.Lett.* **95** 122508

[42] Vafaee M, Finizio S, Deniz H,Hesse D, Zabel H, Jakob G, and Kläui M 2016 The effect of interface roughness on exchange bias in $La_{0.7}Sr_{0.3}MnO_3BiFeO_3$ heterostructures *Appl.Phys.Lett.* **108** 72401

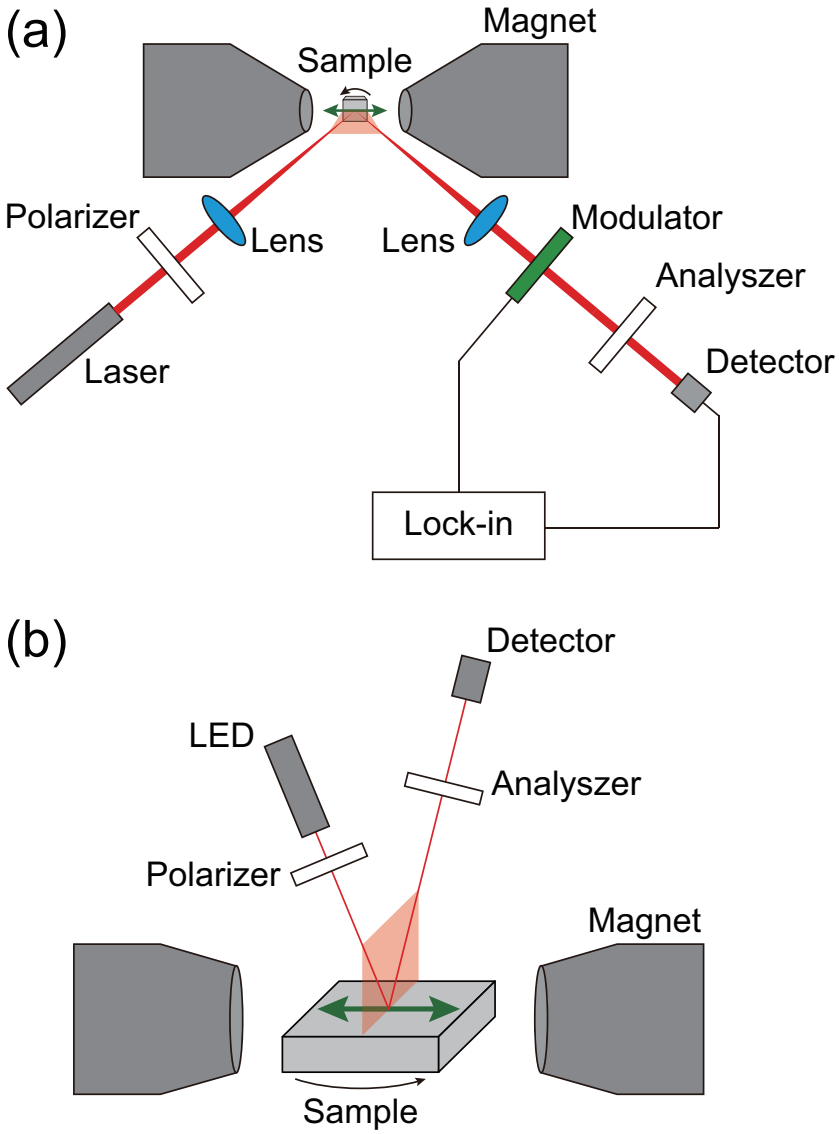

Figure 1. (Color online) Experimental MOKE setups of L-MOKE using laser diode (a) and T-MOKE using Kerr microscope (b).

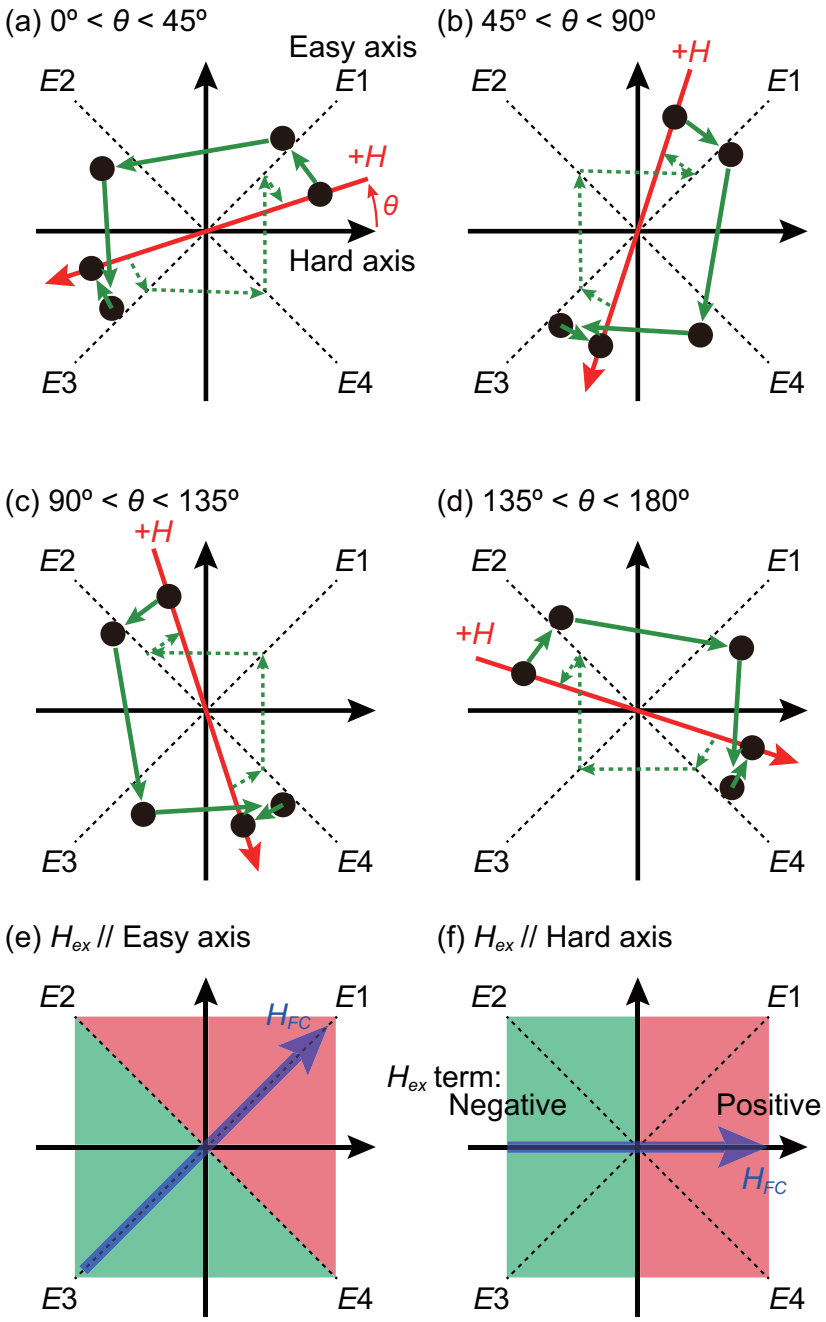

Figure 2. (Color online) (a-d) Schematic magnetization switching process resulting from the fourfold magnetocrystalline anisotropy. (e, f) Sign of exchange-coupling term of Eq. 1 with respect to FC direction parallel to the easy axis E1 along [110] (e) and the hard axis along [100] (f).

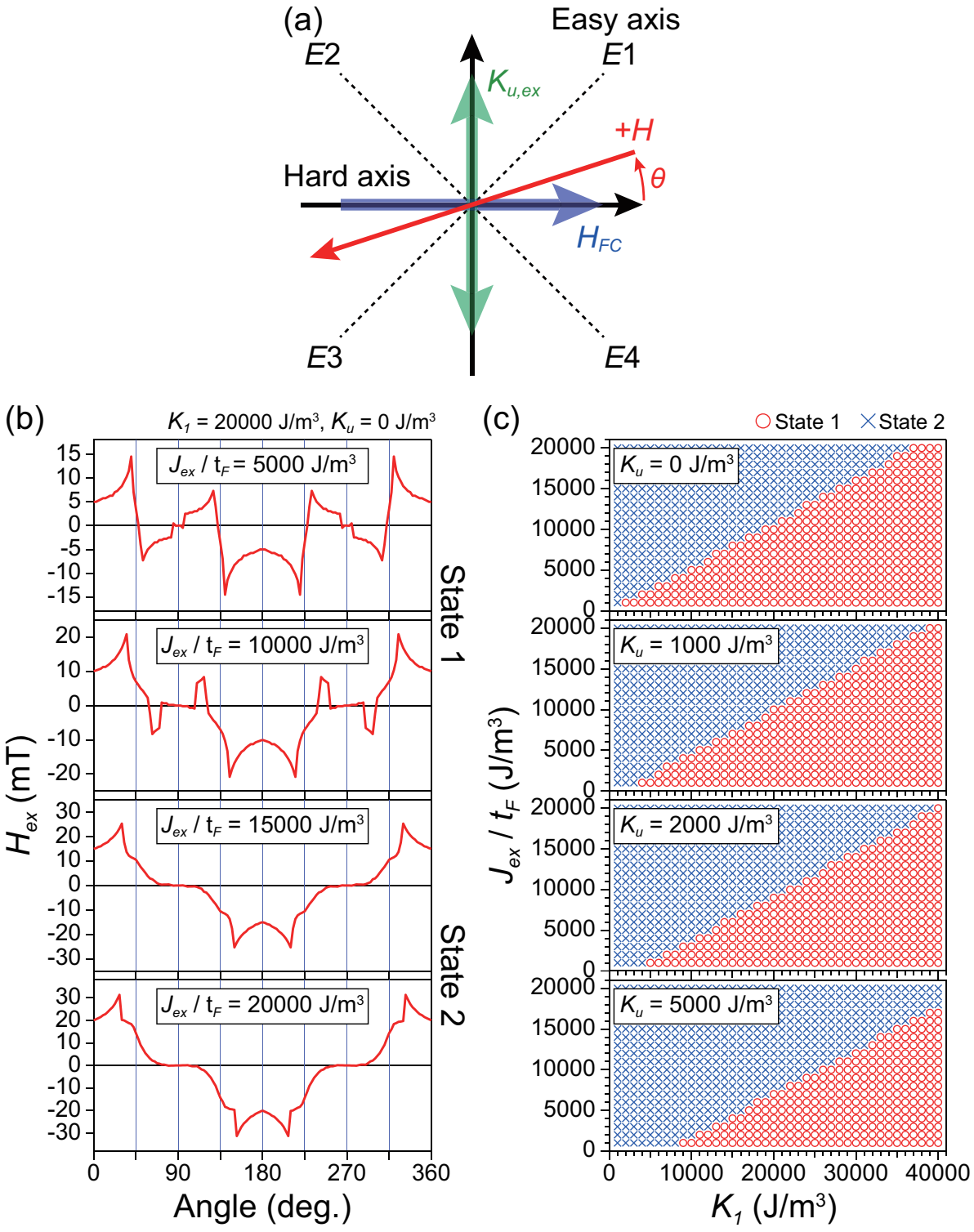

Figure 3. (Color online) (a) Model and experimental configuration. (b) Series of calculated angular-dependent exchange bias as a function of J_{ex}/t_F using $K_1 = 20000$ J/m^3 and $K_u = 0$ J/m^3. (c) Calculated K_1-J_{ex}/t_F phase diagram as a function of K_u.

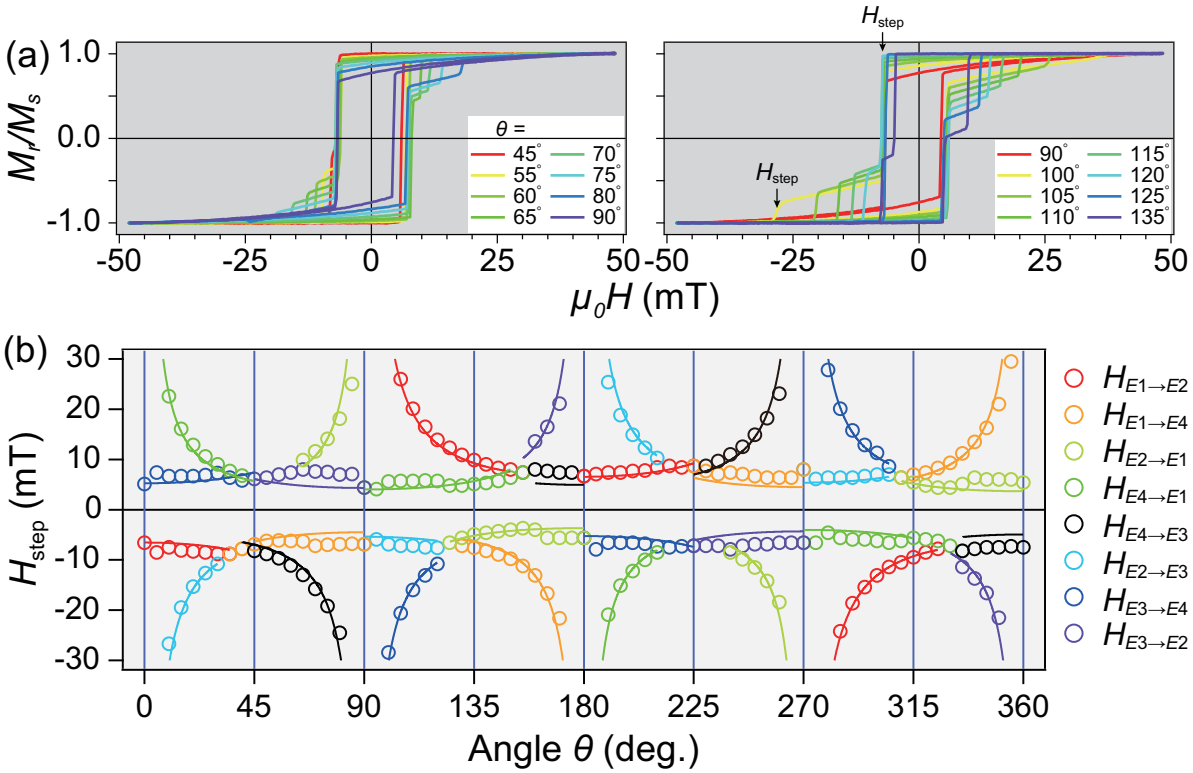

Figure 4. (Color online) (a) Series of angular-dependent L-MOKE loops after FC along $\langle 100 \rangle$ direction. (b) The angular-dependent step positions H_{step} as a function of angle. The open circles and solid lines are experimental data and model fittings, respectively.

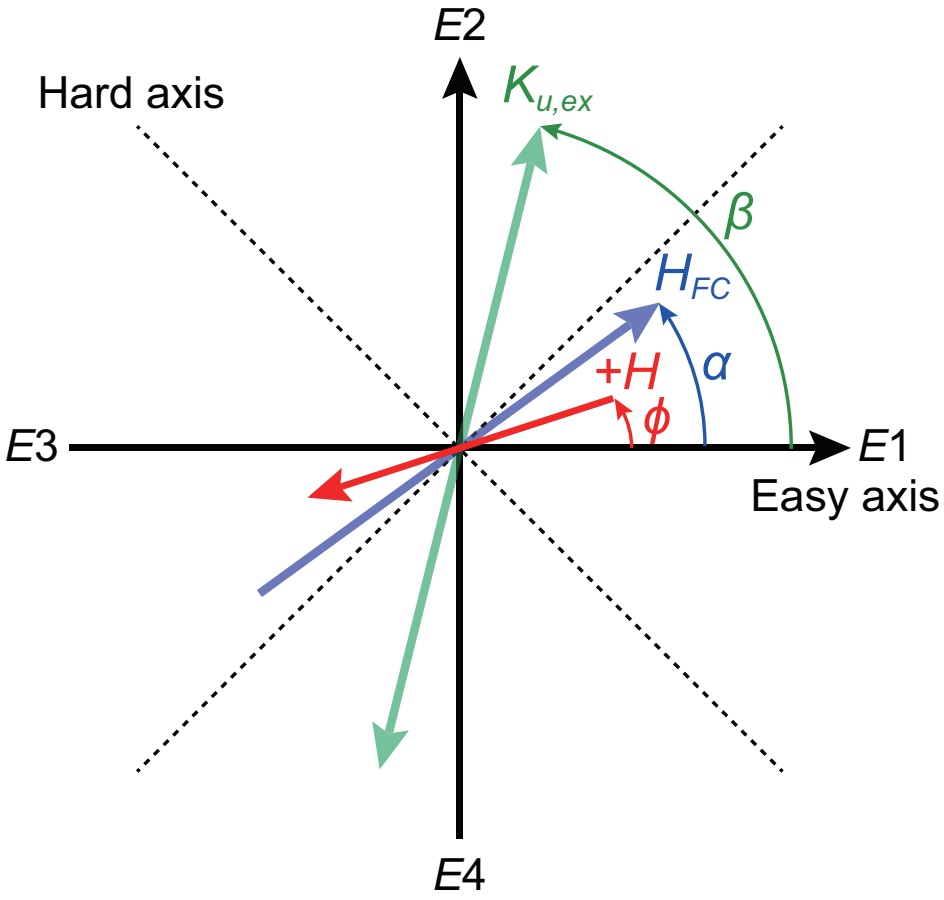

Figure 5. (Color online) Configuration of non-collinear anisotropies case.

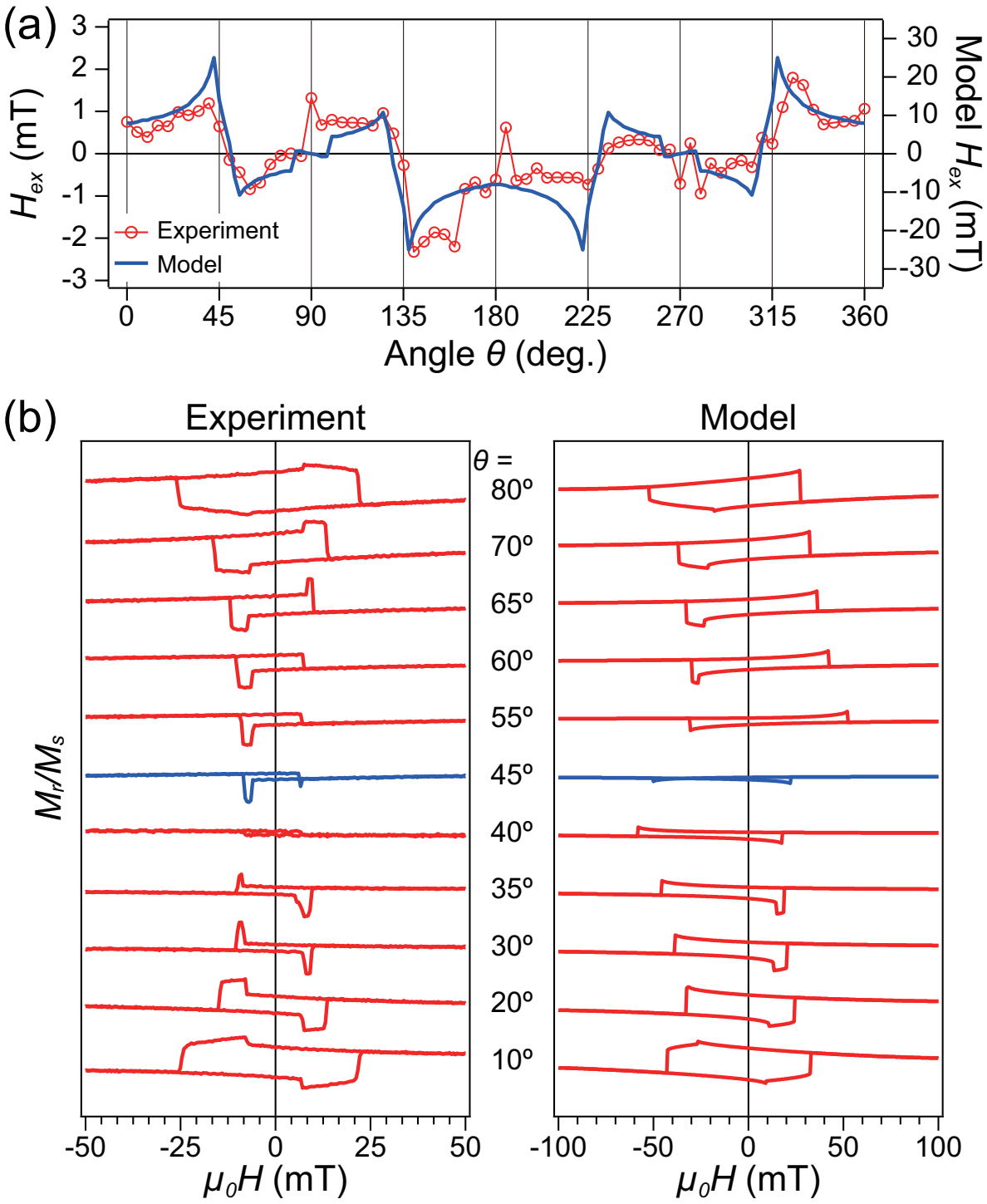

Figure 6. (Color online) Comparison of angular-dependent exchange bias (a) and T-MOKE loops (b) with the model using $K_1 = 33700$ J/m^3, $J_{ex}/t_F = 8000$ J/m^3 and $K_{u,ex} = 2450$ J/m^3.